

Coherent control of nanomagnet dynamics via ultrafast spin torque pulses.

Samir Garzon¹, Longfei Ye¹, Richard A. Webb¹, Thomas M. Crawford¹, Mark Covington² & Shehzaad Kaka²

¹ *Physics and Astronomy Department and USC Nanocenter,
University of South Carolina, Columbia, SC 29208, USA.* ² *Seagate Research,
1251 Waterfront Place, Pittsburgh, Pennsylvania 15222, USA.*

PACS numbers: 72.25.Ba, 73.63.-b, 75.75.+a

The magnetization orientation of a nanoscale ferromagnet can be manipulated using an electric current via the spin transfer effect [1, 2, 3, 4]: spin angular momentum is transferred from the conduction to the localized electrons, exerting an effective torque on the ferromagnet [5, 6, 7, 8]. Time domain measurements of nanopillar devices at low temperatures have directly shown that magnetization dynamics and reversal occur coherently over a timescale of nanoseconds [9]. By adjusting the shape of a spin torque waveform over a timescale comparable to the free precession period (100-400 ps), control of the magnetization dynamics in nanopillar devices should be possible [10, 11, 12]. Here we report coherent control of the free layer magnetization in nanopillar devices using a pair of current pulses as narrow as 30 ps with adjustable amplitudes and delay. We show that the switching probability can be tuned over a broad range by timing the current pulses with the underlying free-precession orbits, and that the magnetization evolution remains coherent for more than 1 ns even at room temperature. Furthermore, we can selectively induce transitions along free-precession orbits and thereby manipulate the free magnetic moment motion. In contrast with previous measurements where the spin torque is applied throughout a large fraction of a precession cycle [13, 14, 15, 16, 17], in our experiments the magnetization evolves through free-precession except for short time intervals when it is driven by the spin torque. We expect this technique will be adopted for further elucidating the dynamics and dissipation processes in nanomagnets, and will provide an alternative for spin torque driven spintronic devices, such as resonantly pumping microwave oscillators [18, 19], and ultimately, for efficient reversal of magnetic memory bits in nanoscale magnetic random access memory (MRAM).

We study spin transfer nanopillar devices patterned into ~ 100 nm ellipses with different aspect ratios (inset of Fig. 1a) at room temperature and 77 K. Antiferromagnetic dipolar field coupling between the thick layer (polarizer) and the “free” layer is canceled by biasing the devices with an easy axis magnetic field $H_{||} \sim 800$

Oe. The “free” layer can be switched between low resistance (parallel, P) and high resistance (anti-parallel, AP) states via a spin-transfer torque from an applied dc current. A simple shaped waveform, consisting of two current pulses with equal polarity, comparable amplitude, and separated by a time delay t_D (inset of Fig. 1b), is used to induce and control nanomagnet dynamics, while the final state of the multilayer is probed by measuring its steady state resistance. In our devices the free precession period $\tau \sim 300$ ps is much larger than the current pulse width $\tau_w \sim 30$ ps FWHM, but comparable to the inter-pulse delay $0 \text{ ns} < t_D < 2 \text{ ns}$. A femtosecond mode-locked laser in single-shot mode is used to generate a pair of optical pulses which are converted to electrical pulses using a LT-GaAs/Au photoconductive switch [20, 21]. A 40 GHz bias tee is used to inject both the current pulses that induce magnetization dynamics and the ac/dc currents used to measure the resistance and reset the device. Reflection measurements show that typical room temperature pulsewidths at the device are ~ 30 ps, but due to cryostat bandwidth limitations the typical pulsewidths are ~ 58 ps at 77 K. At nonzero temperatures thermal excitation of the “free” layer magnetization (\vec{M}) affects its dynamical evolution. However, reproducibility in nanomagnet switching can be increased by applying transverse fields [16] or through inter-layer coupling [9]. Throughout our measurements we apply in-plane transverse fields $H_{\perp} \sim 200$ Oe to shift the stable points of \vec{M} away from the easy axis (inset of Fig. 1a).

The switching probability P_S as a function of inter-pulse delay for equal amplitude pulses at 77 K is shown in Fig. 1a. Large modulation of P_S with delay implies coherent dynamics, since incoherent dynamics would lead to a delay-independent switching probability $P_2 = 1 - (1 - P_1)^2$ (with P_1 the single-pulse switching probability). To understand the origin of these oscillations, we model the time evolution of the magnetization of a single domain nanomagnet driven by a perpendicular spin current (inset of Fig. 1a), by using a modified Landau-Lifshitz-Gilbert equation which includes the Slonczewski spin torque term [2, 22]. We assume that the magnetization of the polarizer is fixed, and consider the effect of nonzero temperatures only on the distribution of initial conditions but not on the evolution of \vec{M} , which is assumed to be completely deterministic. \vec{M} is described by

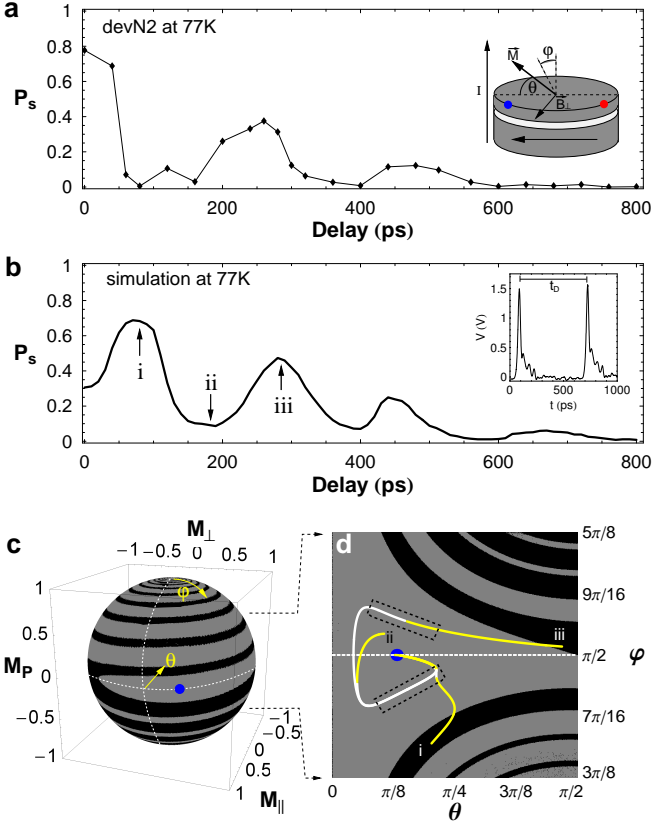


FIG. 1: Modulation of switching probability with delay. **a**, P_S of device N2 at 77 K as a function of delay between two ~ 22 mA current pulses. **Inset**, Schematic of a $\text{Co}_{90}\text{Fe}_{10}(8.7\text{nm})/\text{Cu}(3\text{nm})/\text{Co}_{90}\text{Fe}_{10}(2\text{nm})$ (type “N”) nanopillar device. $[\text{Ni}_{80}\text{Fe}_{20}(20\text{nm})/\text{Co}_{90}\text{Fe}_{10}(2\text{nm})]/\text{Cu}(10\text{nm})/\text{Co}_{90}\text{Fe}_{10}(3\text{nm})$ (type “E”) devices have an extended bottom layer $[\text{NiFe}/\text{CoFe}]$ to decrease magnetic layer dipolar coupling. A transverse field is used to shift the parallel (P) and anti-parallel (AP) fixed points (blue and red dot respectively) away from the easy axis. **b**, Simulation of the delay dependence of the switching probability due to two 58 ps FWHM pulses, for an elliptical free layer of size $125\text{nm} \times 75\text{nm} \times 2\text{nm}$ with saturation magnetization $M_S = 800 \text{ emu/cm}^3$, a Stoner-Wohlfarth switching field $H_k = 200 \text{ Oe}$, and a transverse field $H_{\perp} = 80 \text{ Oe}$ at 77 K. The labeled regions correspond to the orbits shown in Fig. 1d. **Inset**, Pair of ~ 30 ps pulses with a delay $t_D = 700$ ps measured at a pick-off tee before the device. **c**, Phase portrait of \vec{M} showing the basins of attraction for the two stable points P (blue) and AP (red, not visible). Initial conditions θ, φ within the gray (black) basin lead to no-switching (switching). θ is the polar angle measured from the nanomagnet easy axis and φ is the azimuthal angle measured from the normal to the nanomagnet plane shown in the inset of Fig. 1a. **d**, \vec{M} trajectories generated by two current pulses of equal amplitude that have been delayed by 90 ps (i), 190 ps (ii), and 280 ps (iii). The rectangles enclose regions where a second pulse has high probability of switching \vec{M} .

the angles θ and φ (inset of Fig. 1a)[22], and has fixed points at $\varphi = \pi/2$, $\theta = \arcsin H_{\perp}/H_k$ with H_k the easy axis anisotropy field. The phase portrait of \vec{M} in the absence of spin torque is shown in Fig. 1c[23]. The black and gray regions, which are the basins of attraction for the red and blue minimum energy points, are wrapped around each other, emphasizing the final state’s large sensitivity to fluctuations in initial conditions (i.e. thermal effects).

Simulations of the delay dependence of P_S for a pair of pulses with equal amplitude at 77 K (Fig. 1b) show oscillations with delay that agree qualitatively with our observations (Fig. 1a). Typical trajectories at consecutive maxima and minima of P_S , regions labeled i, ii, and iii, in Fig. 1b are shown in Fig. 1d, where the section $3\pi/8 < \varphi < 5\pi/8$ of the phase portrait shown in Fig. 1c has been stretched into a plane. The initial condition and first pulse (in yellow) are equivalent for all trajectories, but the second pulse (also in yellow) is applied at different times ($t_D = 90$ ps, 190 ps, and 280 ps). The free evolution between the two pulses is shown in white. We observe that there are two regions (dashed boxes in Fig. 1d) where the second spin torque pulse can more effectively induce basin boundary crossing and lead to magnetization reversal. As indicated by trajectory ii, a second pulse applied outside of the marked regions can even push \vec{M} closer to the blue fixed point, effectively cancelling the effect of the first pulse. Therefore, when a pulse with a width larger than the free precession period is used for magnetization switching, partial cancellation of the spin torque can occur, decreasing the switching probability.

We observe that the clear oscillations and strong modulation of P_S present in device N2 at 77 K (Fig. 1a) disappear at room temperature (Fig. 2a). Type “N” devices, with dc switching currents ~ 0.4 mA, have a small stability factor $\Delta = E_B/k_B T$ (with E_B the energy barrier between P and AP states), and thus are more sensitive to thermal effects. At room temperature such devices typically show decay in P_S with increasing delay, and small amplitude P_S oscillations. On the other hand, extended bottom layer (type “E”) devices, with switching currents ~ 2 mA and therefore higher thermal stability, typically show clear large amplitude oscillations in P_S both at 77 K (Fig. 2b) and room temperature (Fig. 2c). Fourier analysis of the oscillations of device E1 at 77 K shows a fundamental period of 120 ps ($\omega = 8.3\text{GHz}$) and a much smaller 2ω harmonic. Since the precession period is twice the period of the P_S oscillations, for type “E” devices $\tau \sim 240$ ps. At room temperature the switching probability of device E2 can be tuned between 4% and 93% by only adjusting the delay between pulses. The enhancement in the switching probability from 60% at zero delay (single pulse) to $\sim 94\%$ at 120 ps delay (Fig. 2c) has been measured while keeping the amplitude of the pulses constant. However, if the total energy delivered by the

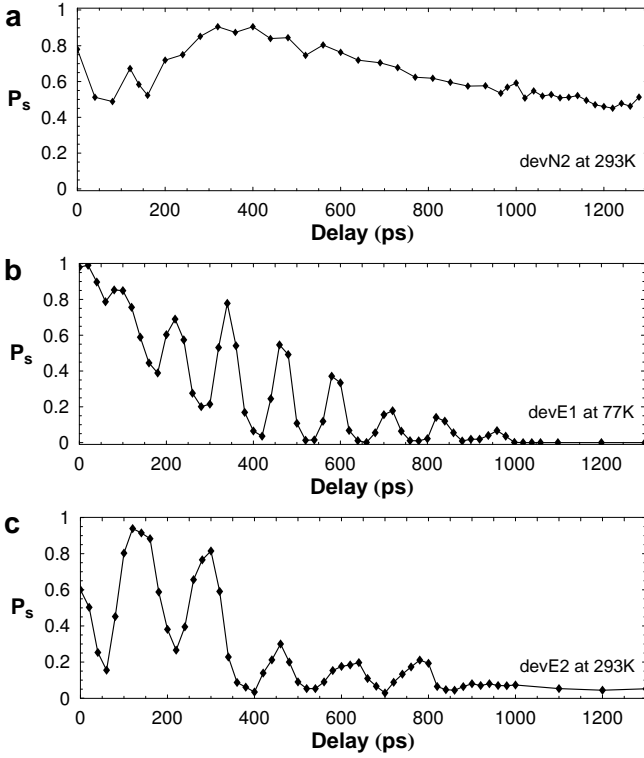


FIG. 2: **Effect of temperature on switching probability modulation.** P_S as a function of delay for: **a**, device N2 at room temperature. **b**, device E1 (with extended bottom layer) at 77 K. **c**, device E2 (with extended bottom layer) at room temperature. Type “E” devices require larger switching currents than type “N” devices due to increased thermal stability. Therefore, large modulation of P_S can be observed in typical type “E” devices even at room temperature.

pulses is kept constant, a more dramatic enhancement in P_S from 10% to 70% at intermediate pulse amplitudes and from 40% to 95% at larger pulse amplitudes is observed. Therefore, multiple current pulses timed with the underlying coherent dynamics require less total energy than a single pulse to reproducibly switch spin transfer devices.

We also measured the switching probability as a function of the amplitude of a pair of pulses while keeping their delay (185 ps) and relative amplitude ($I_1/I_2 = 1$) constant (Fig. 3a). P_S initially increases with increasing pulse amplitude, but after 15 mA it decreases from 80% to 55% before finally increasing to $\sim 100\%$ at 23 mA. This counterintuitive result that increasing the spin torque leads to a decrease in the switching probability is fully consistent with coherent precession and is predicted by our simulations (Fig. 3b). This agreement demonstrates that in our system the macro-spin model captures the essence of nanomagnet dynamics. Typical magnetization trajectories at the three labeled regions of Fig. 3b are shown in Fig. 3c. As the amplitude of the pair of pulses

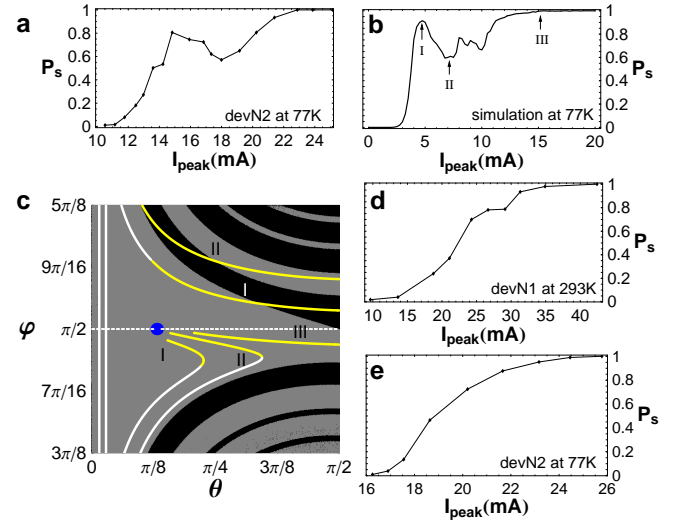


FIG. 3: **Amplitude dependence of the switching probability.** **a**, P_S at 77 K as a function of the amplitude of a pair of ~ 58 ps pulses with a fixed delay of 185 ps, for type “N” device 2. The amplitudes of both pulses are kept equal. **b**, Simulated switching probability for the situation described in **a** for the same parameters as Fig. 1b. **c**, \vec{M} trajectories at the labeled regions of Fig. 3b corresponding to pulse amplitudes of 4.8 mA (I), 6.8 mA (II), and 15 mA (III). Initial conditions have a thermal probability distribution. **d**, P_S at room temperature as a function of the amplitude of a single ~ 30 ps pulse for type “N” device 1. **e**, P_S at 77 K as a function of the amplitude of a single ~ 58 ps pulse for type “N” device 2.

is increased from region I to region II (Fig. 3b), the state of \vec{M} at the end of the second pulse moves from the black basin to a higher energy gray basin region, therefore decreasing P_S (Fig. 3c). As the amplitude of the pulses is increased further to region III in Fig. 3b, the first pulse produces enough spin torque to switch \vec{M} (Fig. 3c). Thus it is possible to move the magnetization into larger angle, higher energy orbits by applying multiple short current pulses with controlled amplitudes and delays.

In contrast to previous reports [13, 14, 15] where single pulses with $\tau_w > 100$ ps were required to achieve large P_S , we demonstrate $P_S \sim 100\%$ with single 30 ps pulses at room temperature (Figs. 3d,e). Furthermore, for devices with dc switching currents comparable to those previously reported [14, 15] we achieve $P_S \approx 100\%$ with pulse amplitudes two times smaller than expected from the assumption of pulsewidth and amplitude being inversely proportional [24, 25]. These results are supported by macrospin simulations which indicate that the pulsewidth-current product required for $P_S = 95\%$ decreases by more than a factor of two when $\tau_w \ll \tau$. Therefore, ultrashort current pulses apply spin torque more efficiently, increasing the probability of magnetization switching. Depending on field bias, temperature, and device anisotropy, P_S can show either stepped [16]

(Fig. 3d) or smooth [14, 15] (Fig. 3e), but always monotonic increase with increasing pulse amplitude. The stepped increase in P_S is predicted by our simulations and was previously observed when increasing the pulse width [16]. The steps are caused by the underlying free precession orbits, which play an essential role at short timescales, where the switching process is driven, instead of thermally-assisted. Thus, the free precession orbits provide a map for tailoring the amplitudes and timing of a series of short pulses in order to control the magnetization evolution.

As long as the motion remains coherent until the arrival of the last pulse, a series of short current pulses can be used to manipulate the free layer into a desired free-precession orbit, that is, to coherently control the magnetization. Our technique not only provides a proof of principle for such pulsed magnetization control, but also demonstrates coherent magnetic moment dynamics even at room temperature, and provides an alternative for high probability low power device switching. Using current pulses much shorter than the free-precession period is critical for controlling the magnetization motion. Our technique can be used to study the switching process in magnetic tunnel junctions, where a quiet “incubation” period that precedes magnetization switching has been observed [17], as well as to probe coherence and damping in out-of-plane nanopillar devices. Potential applications of our approach also include nano-oscillators [18, 19] which could be resonantly pumped for generating tunable microwaves over a broad GHz range.

We acknowledge helpful discussions with Yaroslav Bazaliy. This work was funded by Seagate Research.

-
- [1] J. C. Slonczewski, *Journal of Magnetism and Magnetic Materials* **159**, L1 (1996).
 - [2] J. C. Slonczewski, *Journal of Magnetism and Magnetic Materials* **195**, 261 (1999).
 - [3] L. Berger, *Phys. Rev. B* **54**, 9353 (1996).
 - [4] L. Berger, *Journal of Applied Physics* **49**, 2156 (1978).
 - [5] J. A. Katine, F. J. Albert, R. A. Buhrman, E. B. Myers, and D. C. Ralph, *Phys. Rev. Lett.* **84**, 3149 (2000).
 - [6] J. Z. Sun, *Journal of Magnetism and Magnetic Materials* **202**, 157 (1999).
 - [7] M. Tsoi, A. G. M. Jansen, J. Bass, W.-C. Chiang, M. Seck, V. Tsoi, and P. Wyder, *Phys. Rev. Lett.* **80**, 4281 (1998).
 - [8] E. B. Myers, D. C. Ralph, J. A. Katine, R. N. Louie, and R. A. Buhrman, *Science* **285**, 867 (1999).
 - [9] I. N. Krivorotov, N. C. Emley, J. C. Sankey, S. I. Kiselev, D. C. Ralph, and R. A. Buhrman, *Science* **307**, 228 (2005).
 - [10] K. Rivkin and J. B. Ketterson, *Applied Physics Letters* **88**, 192515 (pages 3) (2006).
 - [11] L. Thomas, M. Hayashi, X. Jiang, R. Moriya, C. Rettner, and S. Parkin, *Nature* **443**, 197 (2006).
 - [12] L. Thomas, M. Hayashi, X. Jiang, R. Moriya, C. Rettner, and S. Parkin, *Science* **315**, 1553 (2007).
 - [13] A. A. Tulapurkar, T. Devolder, K. Yagami, P. Crozat, C. Chappert, A. Fukushima, and Y. Suzuki, *Applied Physics Letters* **85**, 5358 (2004).
 - [14] S. Kaka, M. R. Pufall, W. H. Rippard, T. J. Silva, S. E. Russek, J. A. Katine, and M. Carey, *Journal of Magnetism and Magnetic Materials* **286**, 375 (2005).
 - [15] M. L. Schneider, M. R. Pufall, W. H. Rippard, S. E. Russek, and J. A. Katine, *Applied Physics Letters* **90**, 092504 (pages 3) (2007).
 - [16] T. Devolder, C. Chappert, J. A. Katine, M. J. Carey, and K. Ito, *Physical Review B (Condensed Matter and Materials Physics)* **75**, 064402 (pages 5) (2007).
 - [17] T. Devolder, J. Hayakawa, K. Ito, H. Takahashi, S. Ikeda, P. Crozat, N. Zerounian, J.-V. Kim, C. Chappert, and H. Ohno, *Physical Review Letters* **100**, 057206 (pages 4) (2008).
 - [18] W. H. Rippard, M. R. Pufall, S. Kaka, S. E. Russek, and T. J. Silva, *Physical Review Letters* **92**, 027201 (pages 4) (2004).
 - [19] S. Kaka, M. Pufall, W. Rippard, T. Silva, S. Russek, and J. Katine, *Nature* **437**, 389 (2005).
 - [20] D. H. Auston, in *Picosecond Optoelectronic Devices*, edited by C. H. Lee (Academic, Orlando, 1984), pp. 73–117.
 - [21] F. W. Smith, H. Q. Le, V. Diadiuk, M. A. Hollis, A. R. Calawa, S. Gupta, M. Frankel, D. R. Dykaar, G. A. Mourou, and T. Y. Hsiang, *Applied Physics Letters* **54**, 890 (1989).
 - [22] J. Z. Sun, *Phys. Rev. B* **62**, 570 (2000).
 - [23] Y. B. Bazaliy, B. A. Jones, and S.-C. Zhang, *Phys. Rev. B* **69**, 094421 (2004).
 - [24] R. H. Koch, J. A. Katine, and J. Z. Sun, *Physical Review Letters* **92**, 088302 (2004).
 - [25] Z. Li and S. Zhang, *Phys. Rev. B* **68**, 024404 (2003).